Available online at www.sciencedirect.com

SCIENCE DIRECT

Developmental Biology 283 (2005) 409 – 423

DEVELOPMENTAL BIOLOGY

www.elsevier.com/locate/ydbio

Functional analyses in the milkweed bug *Oncopeltus fasciatus* (Hemiptera) support a role for Wnt signaling in body segmentation but not appendage development

David R. Angelini[1], Thomas C. Kaufman*

Department of Biology, Indiana University, 1001 E. Third Street, Bloomington, IN 47405-7005, USA

Received for publication 21 January 2005, revised 29 April 2005, accepted 29 April 2005
Available online 4 June 2005

Abstract

Specification of the proximal–distal (PD) axis of insect appendages is best understood in *Drosophila melanogaster*, where conserved signaling molecules encoded by the genes *decapentaplegic* (*dpp*) and *wingless* (*wg*) play key roles. However, the development of appendages from imaginal discs as in *Drosophila* is a derived state, while more basal insects produce appendages from embryonic limb buds. Therefore, the universality of the *Drosophila* limb PD axis specification mechanism has been debated since *dpp* expression in more basal insect species differs dramatically from *Drosophila*. Here, we test the function of Wnt signaling in the development of the milkweed bug *Oncopeltus fasciatus*, a species with the basal state of appendage development from limb buds. RNA interference of *wg* and *pangolin* (*pan*) produce defects in the germband and eyes, but not in the appendages. *Distal-less* and *dachshund*, two genes regulated by Wg signaling in *Drosophila* and expressed in specific PD domains along the limbs of both species, are expressed normally in the limbs of *pan*-depleted *Oncopeltus* embryos. Despite these apparently paradoxical results, Armadillo protein, the transducer of Wnt signaling, does not accumulate properly in the nuclei of cells in the legs of *pan*-depleted embryos. In contrast, *engrailed* RNAi in *Oncopeltus* produces cuticular and appendage defects similar to *Drosophila*. Therefore, our data suggest that Wg signaling is functionally conserved in the development of the germband, while it is not essential in the specification of the limb PD axis in *Oncopeltus* and perhaps basal insects.

Keywords: *Oncopeltus*; Milkweed bug; Hemiptera; *Wingless*; *Pangolin*; *Decapentaplegic*; *Engrailed*; RNA interference; Appendage patterning

Introduction

Appendages are present in several of the most successful animal groups, and they are a defining feature of the arthropods. Much of our understanding of appendage development has been taken from the foremost model arthropod, the fruit fly *Drosophila melanogaster* (Diptera). However, the universality of *Drosophila* appendage-patterning mechanisms is questionable, particularly given the derived nature of limb development from imaginal discs in *Drosophila*. Imaginal discs are epithelial sheets of cells set-aside during embryogenesis but patterned during larval development. These structures are unique to the Holometabola, but appendage development from imaginal discs is not universal among this group. In Coleoptera, Trichoptera, Neuroptera, and Lepidoptera, only some adult appendage types develop from imaginal discs (Svacha, 1992), while the phenomenon is most pronounced in the cyclorhaphous Diptera, where all adult appendages are produced from imaginal discs. In contrast, limb development in most insect orders proceeds directly from three-dimensional embryonic limb buds. Given these differences of topology, potential differences in the specification of the limb proximal–distal (PD) axis are possible.

In *Drosophila*, the adult appendages develop from imaginal discs during the larval stages. The discs are sheets

* Corresponding author.
E-mail address: kaufman@bio.indiana.edu (T.C. Kaufman).
[1] Present address: University of Connecticut, Department of Ecology and Evolutionary Biology, 75 N. Eagleville Road U-3043, Storrs, CT 06269-3043, USA.

0012-1606/$ - see front matter © 2005 Elsevier Inc. All rights reserved.
doi:10.1016/j.ydbio.2005.04.034

of epithelia, in which the central and presumptively distal region of the limb telescopes out during pupal development to yield the mature appendages. However, larval patterning of the disc occurs in an essentially two-dimensional sheet of cells.

The specification of the limb PD axis is best understood in the leg disc, where it is defined by the overlap of signaling molecules encoded by the genes *decapentaplegic* (*dpp*) and *wingless* (*wg*). In the embryo, *wg* is required for the formation of the imaginal disc primordia (Kubota et al., 2003; Simcox et al., 1989). Removal of *wg* activity during this period eliminates the appendages and other imaginal disc derivatives (Cohen et al., 1993). In the imaginal leg disc, *dpp* and *wg* are expressed in stripes along the anterior–posterior (AP) compartment boundary on the dorsal and ventral sides, respectively (Baker, 1988a; Masucci et al., 1990), in response to activation by *hedgehog* signaling from the posterior compartment (Diaz-Benjumea et al., 1994). *wg* encodes a secreted Wnt signaling molecule (Rijsewijk et al., 1987) that also acts as a segment polarity gene in the germband (Ingham and Martinez-Arías, 1992). Similarly, *dpp* encodes a signaling molecule of the TGF-β protein family (Padgett et al., 1987), which also acts to establish the dorsal–ventral (DV) body axis (Irish and Gelbart, 1987). The imaginal leg disc is an essentially two-dimensional structure in which these signaling pathways interact. In this context, Dpp and Wg signaling mutually inhibit one another's expression to define dorsal and ventral territories of the disc, respectively (Theisen et al., 1996). Because of the two-dimensional character of the imaginal disc, Wg and Dpp ligands overlap in a graded manner only at its center. There, they cooperatively activate distal appendage-patterning genes, such as *Distal-less* (*Dll*) and *dachshund* (*dac*), while repressing proximal genes such as *homothorax* (*hth*) (Abu-Shaar and Mann, 1998; Diaz-Benjumea et al., 1994; Lecuit and Cohen, 1997). In this way, *wg* and *dpp* cooperate to specify the first distinct domains along the limb PD axis.

In contrast to *Drosophila*, most other arthropods produce appendages directly from embryonic limb buds. A consistent and interesting theme has emerged from studies reporting the expression patterns of appendage-patterning orthologues in non-model species. Generally, the expression of PD domain genes, such as *Dll* and *dac*, is well conserved, in discrete regions of the legs (Abzhanov and Kaufman, 2000; Angelini and Kaufman, 2004; Prpic and Tautz, 2003; Prpic et al., 2003). Similarly, the expression of *wg* orthologues appears conserved. In the red flour beetle *Triboliumcastaneum* (Nagy and Carroll, 1994), the cricket *Gryllus bimaculatus* (Miyawaki et al., 2004), and the spider *Cupiennius salei* (Prpic et al., 2003), *wg* expression extends in stripes along the parasegmental compartment boundaries into the limb buds to their distal tips. However, *dpp* orthologues examined in other arthropods show a pattern that is unlike *Drosophila* but fairly consistent among the diverse species examined. In species, such as *Tribolium* (Sanchez-Salazar et al., 1996), the grasshopper *Schistocerca americana* (Jockusch et al., 2000), and *Cupiennius* (Prpic et al., 2003), early *dpp* expression appears throughout the limb buds. As the limb buds elongate, rings of expression are formed at or just proximal of the distal tip. Later, additional weaker rings of expression appear at different PD levels along the legs of *Schistocerca* and *Cupiennius*.

The differences in *dpp* expression between *Drosophila* and other arthropods are striking and imply perhaps different modes of action in the specification of the limb PD axis for *Drosophila* as compared to more basal insects. However, a model has recently been proposed by Prpic et al. (2003), based on comparative data and mathematical models of the *Drosophila* imaginal leg disc (Almirantis and Papageorgiou, 1999). These authors have noted that because Wg and Dpp cooperate to active distal targets, it is crucial that these ligands remain spatially separated in areas fated to become proximal, where Wg and Dpp proteins should not co-occur. Since *dpp* and *wg* are expressed in separate DV territories of the anterior compartment of the *Drosophila* imaginal disc, the ligands cannot diffuse to all proximal areas of the disc, only those in their respective territory. Therefore, stripes of *wg* and *dpp* expression along the compartment boundary in different DV territories allow them to cooperatively activate distal target genes only in the central region of the disc. However, in a three-dimensional limb bud, the dorsal and ventral sides of the proximal limb bud are close enough spatially that the same pattern of *wg* and *dpp* stripes would activate distal target genes over too great a length of the limb bud. This model rationalizes the pattern of distal *dpp* rings in basal insects based on topology. If *dpp* is expressed distally, Wg and Dpp should only overlap in a distal area, and their combined concentration is thought to diminish proximally. Therefore, it is assumed that primitive insects share the same regulatory network architecture as *Drosophila*, in which overlap of Wg and Dpp ligands activates target genes, while inhibiting genes responsible for proximal limb fate.

The topology model, as we shall refer to it, is based on two assumptions: 1 The expression of *wg* and *dpp* in the limb buds of basal insects should be critical to the proper development of appendages in these species. 2. The genetic pathway of the *Drosophila* limb PD axis specification mechanism is conserved. That is, in basal insects, as in *Drosophila*, Wg and Dpp signaling should cooperate to activate distal targets, such as *Dll* and *dac*, while repressing proximal domain genes. Therefore, the topology model leads to at least two testable hypotheses: 1. Perturbations of Wg signaling in basal insects should produce appendage phenotypes similar to those seen in *Drosophila*. 2. The proper expression of genes, such as *Dll* and *dac*, along the limb PD axis of basal insects should require Wg and Dpp signaling.

Here, we test these hypotheses through functional analysis in a hemimetabolous insect, *Oncopeltus fasciatus* (Hemiptera). *Oncopeltus* is a member of the sister taxon to the Holometabola and therefore provides an important

species for comparisons of limb development between hemi- and holometabolous insects. Functional analysis of gene activity is possible in *Oncopeltus* using RNA inference. We present RNAi data for *dpp* and *wg*, as well as *pangolin* (*pan*), the transducer of canonical Wnt signaling (Brunner et al., 1997). Because Wnt signaling also acts in development of the germband and segment polarity, we have also analyzed RNAi of *engrailed* (*en*). Engrailed protein correlates with the anterior parasegmental compartment in *Oncopeltus* (Campbell and Caveney, 1989; Lawrence and Wright, 1981), as in *Drosophila*, where it interacts with *wg* in germband segmentation (Ingham and Martinez-Arías, 1992). Our results suggest that limb PD axis specification in *Oncopeltus* does not depend on the action of Wg signaling. Therefore, we must question the universality of the topological model of appendage development. However, we also note that *Oncopeltus* Wg signaling is conserved in its roles in segment polarity and eye development, as understood from *Drosophila*.

Materials and methods

Insect husbandry and embryology

Large milkweed bugs, *O. fasciatus* (Dallas), were cultured as described previously (Hughes and Kaufman, 2000). Embryos were raised at 25°C for all experiments. At this temperature, embryos hatch after 8 days of development. The germband becomes apparent by approximately 44 h of embryogenesis. In the early *Oncopeltus* germband, the segmental and parasegmental compartments are visible as large (posterior parasegmental) and small (anterior parasegmental) hemisegments. This structure was used to determine the register of segmentally reiterated gene expression patterns.

Sytox staining

Early blastoderm stage embryos were examined after treatment with the fluorescent DNA stain Sytox (Molecular Probes). Embryos were dechorionated and fixed as previously described (Liu and Kaufman, 2004b) then equilibrated in 1 mM EDTA, 0.1% Tween-20 in 10 mM Tris buffer, pH 8.0 (TEw). Embryos were stained in a 1:3000 solution of Sytox in TEw for 30 min with gentle rocking. They were finally de-stained in TEw for at least 30 min.

Immunohistochemistry

Localization of Armadillo (Arm) protein in *Oncopeltus* embryos was determined using the N2 7A1 anti-Arm antibody (Developmental Studies Hybridoma Bank). Embryos were washed in PBS with 0.1% Triton X-100 (PBTx) three times then rocked in 0.2% BSA, PBTx for 30 min. This was followed by 1 h pre-incubation in a blocking agent consisting of 0.2% BSA and 5% normal serum in PBTx. Antibody was added to blocking agent and incubated with embryos for approximately 32 h at 4°C in 5% DMSO and 150 μg/ml RNase (Qiagen). Excess antibody was removed in three washes of 0.2% BSA, PBTx. Embryos were then soaked in 0.2% BSA, PBTx twice for 20 min, then washed again twice in 0.2% BSA, PBTx. Embryos were then pre-incubated in blocking agent for 30 min. The secondary FITC-labeled anti-mouse antibody (Jackson Labs) was incubated overnight at 4°C, with 0.1% TOTO-3 (Molecular Probes, Inc.) to counter-stain DNA. Excess label was removed in three washes in 0.2% BSA, PBTx, and three

Table 1
Phenotypic effects of RNA interference

dsRNA	Mode	Wild type	Specific phenotype				Germband not formed	Pleiotropic defects	Total number
			Total	Class I	Class II	Class III			
dpp	Maternal	–	100%				100%	–	123
en	Zygotic	38%	38%	25%	8%	6%	19%	4%	612
wg	Zygotic	16%	18%				49%	16%	97
	Maternal	93%	–				2%	4%	123
	Total	60%	8%				23%	10%	220
pan	Zygotic	9%	14%	3%	6%	5%	49%	29%	80
	Maternal	–	57%	5%	50%	2%	43%	–	596
	Total	1%	52%	5%	45%	2%	43%	3%	676
control	Zygotic[a]	38%	–				46%	16%	518
	Maternal[b]	93%	–				6%	1%	1437
	Total	79%	–				17%	3%	1955

Listed here are the percentages of individuals displaying various morphologies as a result of dsRNA sequences introduced through zygotic or maternal injection modes. Specific phenotypic effects are divided into classes of severity, where useful, and described in the text. Percentages for phenotypic classes are given out of the total number of embryos displaying a phenotype for that gene and injection method. Totals for both dsRNA delivery methods are listed below those of individual methods. The total number of embryos scored for each dsRNA sequence and injection method is given in the righthand column. Percentages of control experiments are listed here for comparison.

[a] We have previously reported phenotypic percentages for zygotic injection controls (Angelini et al., submitted for publication; Hughes and Kaufman, 2000). The later controls were preformed in conjunction with the experiments of this present study.

[b] Percentages for phenotypes of maternal control injections have also previously appeared (Angelini and Kaufman, 2004).

washes in PBTx. Embryos were then mounted in glycerol with 0.2 M *N*-propylgallate. Imaging was carried out on a Leica DMR confocal microscope.

Isolation of orthologous genes

RNA extraction and cDNA synthesis were used to prepare *Oncopeltus* transcripts for degenerate PCR and RACE, as described previously (Angelini and Kaufman, 2004). Degenerate primers were designed for conserved regions of each gene, and the orthology of cloned sequenced fragments was determined using NCBI BLAST. In this manner, gene fragments of suitable size for in situ hybridization and RNAi were obtained for *Of'dpp* and *Of'pan*. Additional *Of'wg* sequence was isolated through 3′ RACE. Primer sequences are available on request. Sequence data have been submitted to GenBank (AY899334–AY899336).

In situ hybridization

Embryo collection, fixation, and in situ hybridization were performed as previously reported (Liu and Kaufman, 2004b). Antisense RNA probes were synthesized with digoxigenin-labeled uracil. Hybridization to complementary transcripts was detected with an anti-digoxigenin, alkaline phosphatase-conjugated antibody F_{ab}-fragments (Roche), and the chromagens 5-bromo-4-chloro-3-indolyl-phosphate (BCIP; Boerhringer) and nitro-blue-tetrazolium chloride (NBT; Boerhringer). Stained embryos were mounted in Aqua Poly/Mount (Polysciences, Inc.) for imaging.

RNA interference

RNA interference was performed by injecting double-stranded RNA into newly oviposited embryos (zygotic RNAi) or into females (maternal RNAi) as previously described (Angelini and Kaufman, 2004; Hughes and Kaufman, 2000; Liu and Kaufman, 2004a). Both zygotic and parental injections produced similar phenotypes. Table 1 lists the proportions of scored individuals exhibiting various phenotypes for each gene and injection mode.

Microscopy and imaging

Photomicrographs of Sytox-stained blastoderm stage embryos, hatchlings, and 7- to 8-day embryos were taken with a Nikon DXM1200 digital camera on a Nikon SMZ1500 dissecting microscope equipped with a mercury

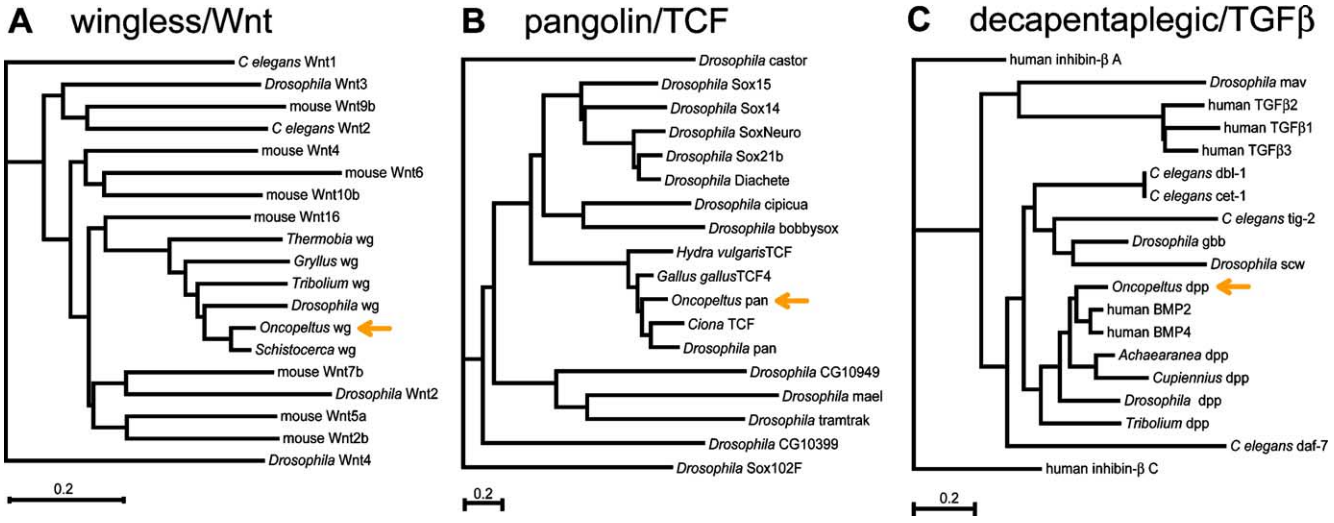

Fig. 1. Unrooted neighbor-joining best trees produced using MacVector 7.2. Sequences were aligned by ClustalW. Distance was Poisson-corrected, and gaps were distributed proportionally. Arrows indicate the position of Oncopeltus orthologues. Which consistently group with orthologues from Drosophila and other insects, to the exclusion of other members of each gene family. For Wg/Wnt orthologues, the aligned area corresponds to the entire fragment of Of'Wg (AY899335) and amino acids 390–468 of Drosophila Wg (AAA28647). GenBank accession numbers of other Wg/Wnt sequences: *C. elegans* Wnt1 (P34888); *Drosophila* Wnt3 (CAA46002); mouse Wnt9b (O35468); *C. elegans* Wnt2 (P34889); mouse Wnt4 (P22724); mouse Wnt6 (P22727); mouse Wnt10b (AAB08087); mouse Wnt16 (Q9QYS1); Thermobia Wg (AF214035); Gryllus Wg (BAB19660); Tribolium Wg (AAB29938); Schistocerca Wg (AAD37798); mouse Wnt7b (AAH58398); *Drosophila* Wnt2 (S24559); mouse Wnt5a (AAH18425); mouse Wnt2b (O70283); *Drosophila* Wnt4 (AAN04479). For Pan/TCF orthologues the aligned area corresponds to the entire fragment of Of'Pan (AY899336) and amino acids 287–373 of Drosophila Pan (P91943). GenBank accession numbers of other HMG-box protein sequences: *Drosophila* Castor (JH0797); *Drosophila* Sox15 (CAB63944); *Drosophila* Sox14 (P40656); *Drosophila* SoxNeuro (CAB64386); *Drosophila* Sox21b (NP_648695); *Drosophila* Diachete (NP_524066); *Drosophila* Cipicua (NP_524992); *Drosophila* Bobbysox (NP_728420); *Hydra vulgaris* TCF (AAG13664); *Gallus gallus* TCF4 (BAA92881); *Ciona savignyi* TCF (BAB68354); *Drosophila* CG10949 (NP_610032); *Drosophila* Maelstrom (AAB97831); *Drosophila* Tramtrak (NP_733446); *Drosophila* CG10399 (NP_609089); *Drosophila* Sox102F (NP_726612). For Dpp/TGFβ orthologues, the aligned area corresponds to the entire Of'Dpp fragment (AY899334) and amino acids 510–581 of *Drosophila* Dpp (P07713). GenBank accession numbers of other Dpp/TGFβ sequences: human Inhibin-βA (NP_002183); *Drosophila* Maverick (AAF99658); human TGFβ2 (NP_003229); human TGFβ1 (NP_000651); human TGFβ3 (NP_003230); *C. elegans* Dbl-1 (NP_504709); *C. elegans* Cet-1 (T43286); *C. elegans* Tig-2 (NP_504271); *Drosophila* Gbb (AAA28307); *Drosophila* Scw (AAA56872); human BMP2 (P12643); human BMP4 (BAA06410); Achaearanea Dpp (BAC24087); Cupiennius Dpp (CAD57730); Tribolium Dpp (Q26974); *C. elegans* Daf-1 (NP_497265); human Inhibin-βC (NP_005529).

light source or a Leica MZ16 automated dissecting microscope. Younger germband embryos were photographed using a Nikon DXM12000 digital camera on a Zeiss Axiophot microscope. Scanning electron micrographs were produced using a Jeol JSM-5800LV electron microscope.

Results

Orthologous gene sequences

Oncopeltus orthologues of *wg*, *pan* and *dpp* were cloned from embryonic cDNA using standard methods. No duplicates or transcriptional isoforms of any of the genes analyzed here were obtained. The orthology of clones was initially determined using NCBI BLAST. However, because these genes are members of large gene families, we verified individual orthologies through the construction of gene phylogenies. For each gene family (Wnt, HMG-box, and TGF-β), orthologous sequences from mammalian and insect model species were aligned with fragments from *Oncopeltus* using ClustalW. The corresponding region of each sequence was used to produce a neighbor-joining tree (Figs. 1A–C). *Oncopeltus* clones were most closely related to *Drosophila wg*, *pan*, and *dpp*, and orthologues of these genes from other species formed clades exclusive of other family members. These clades were still recovered with bootstrap values up to 10,000 (not shown). Therefore, we feel confident in these assignments of orthology.

Expression of Oncopeltus dpp

In *Oncopeltus*, the expression of *dpp* is highly dynamic. Before germband invagination, at 40 h, *dpp* is expressed in an area of the egg posterior (Figs. 2A–B), where invagination will occur (Butt, 1949). In the early germband, *dpp* is expressed in segmentally reiterated stripes, anterior of the parasegment boundary (Fig. 2C). Later, expression at the parasegment boundary disappears, and as limb buds appear, *dpp* is expressed throughout the appendages (Fig. 2D). By 72 h, this expression resolves into a narrow ring near the distal tip of the legs (Fig. 2E). However, *dpp* persists throughout the gnathal appendages. In the antennae, expression is strongest in the distal-most podomere. At 95 h, multiple weak rings of *dpp* expression can be seen in several places along the PD axis of the legs and labial appendages (Figs. 2F–G), although this does not seem to correlate with the position of joints. Expression in the antennae is reduced at this stage and forms a ring near the base of the distal podomere.

This pattern in the limbs differs significantly from the dorsal stripe of expression seen in *Drosophila* leg imaginal discs. However, similar patterns have been reported for other arthropods. For the grasshopper *S. americana* (Jockusch et al., 2000) and the spider *C. salei* (Prpic et al., 2003), *dpp* expression has also been shown to appear in a series of rings late in leg development, around the stages when joints become discernible.

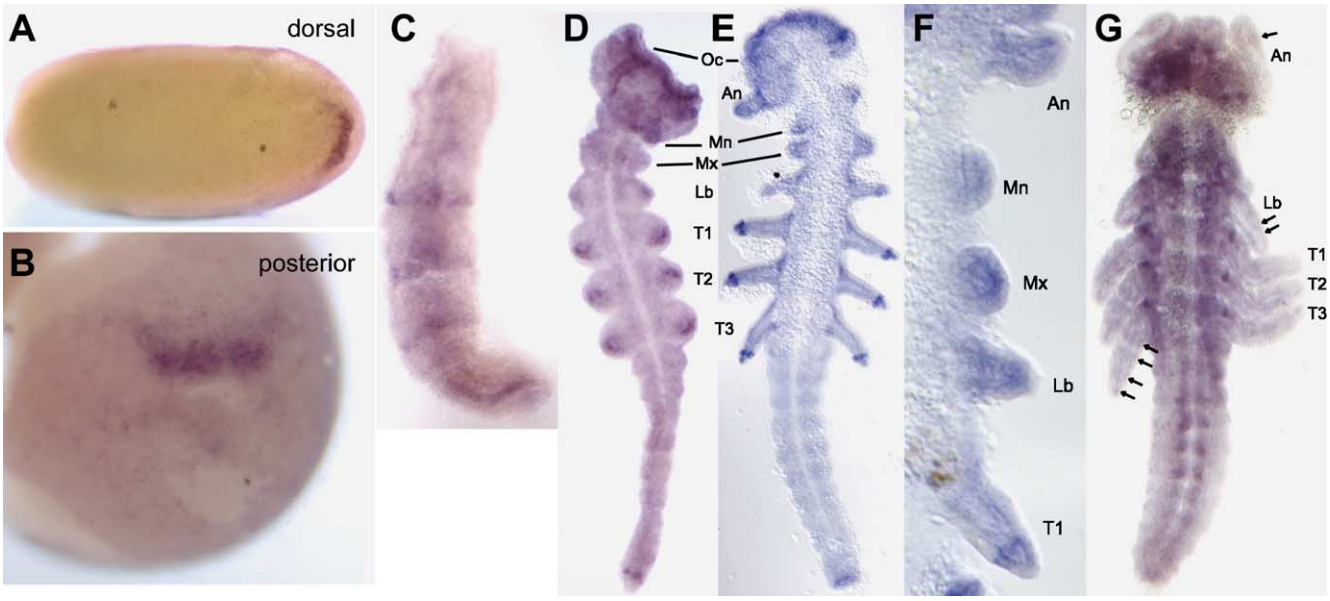

Fig. 2. Expression of *dpp* in *Oncopeltus*. (A) Dorsal view of a 40 h blastoderm stage embryo. *dpp* is expressed along the dorsal edge of the site of germband invagination. (B) Posterior view of a similar embryo. (C) *dpp* is expressed in segmental stripes in a 48 h germband embryo on the anterior side of the parasegment boundary. (D) In a 62 h embryo, *dpp* expression is strongest in the limb buds and ocular segment. (E) *dpp* expression in a 72 h embryo. (F) A similar embryo in close-up, showing that *dpp* is expressed differently in specific appendage types. In the legs, it is restricted to distal rings. (G) By 96 h, *dpp* is expressed extensively in the presumptive nervous system and appears in a series of rings in the appendages (arrows). Abbreviations: Oc, ocular segment; An, antennal segment; Mn, mandibular segment; Mx, maxillary segment; Lb, labial segment; T1–3, thoracic segments 1–3; A1–11, abdominal segments 1–11.

RNA interference of dpp blocks germband invagination

To examine the function of Dpp signaling in *Oncopeltus*, we depleted *dpp* activity through RNA interference. This experiment yielded embryos that failed to produce a germband. At the posterior of the egg, cells normally condense and invaginate to form the germband around 40 h of development (Fig. 3A; Butt, 1949). However, in *dpp*-depleted embryos, these cells condense but do not invaginate (Figs. 3B–C). Later embryonic processes fail to initiate. This phenotype suggests a requirement for Dpp function in germband invagination, but it is not informative regarding the development of appendages. Therefore, we will not consider *dpp* function further in this study.

engrailed RNAi disrupts body segment boundaries and causes appendage deformities and bifurcation

In addition to its function in specifying the limb PD axes, *wg* is also required early in a feed-forward loop with *en*

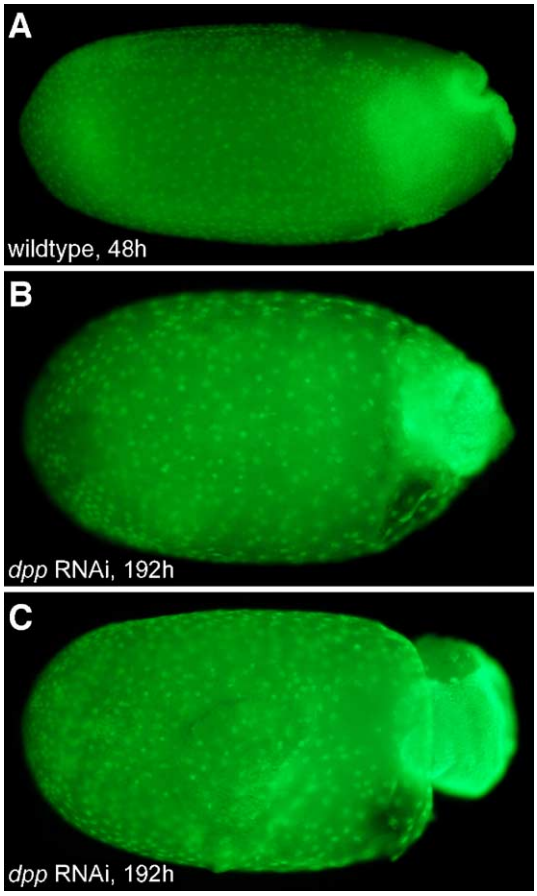

Fig. 3. Of'*dpp* RNAi prevents germband invagination. Sytox-stained embryos are shown with the anterior of the egg to the left. (A) Germband invagination takes place at the posterior of the egg in wild type, as shown in this 48 h embryo. (B) Embryos depleted for *dpp* do not progress beyond this stage even at 192 h (8 days) when embryos normally hatch. Here, cells have condensed at the posterior but failed to invaginate. (C) An embryo in which an apparent attempt at invagination has extended around the embryo, pinching off the posterior region.

(Ingham and Martinez-Arías, 1992), which helps to establish the parasegmental boundary. Specifically, *wg* and *en* activity are required at the anterior and posterior sides of the border, respectively, for establishment of parasegmental boundaries. However, at later stages, including during imaginal disc patterning, *wg* and *en* function independently (Bejsovec and Martinez Arias, 1991). In the imaginal leg disc, *en* expression extends in a band that runs along the posterior side of the AP compartment boundary crossing both the ventral and dorsal territories. Transplantation experiments have suggested a similar role for *en* in establishment of the parasegment boundary in *Oncopeltus* (Campbell and Caveney, 1989), and its expression in the limbs resembles that of *Drosophila* (Rogers and Kaufman, 1997). In order to help distinguish *wg* phenotypes related to segmentation from those related to limb PD axis specification, we first examined the role of *engrailed* (*en*) in these processes. As noted, the expression pattern of *Of'en* has been reported in the limbs where it accumulates throughout the ectoderm of the posterior segmental compartment on the posterior side of the parasegmental boundary (Campbell and Caveney, 1989; Liu and Kaufman, 2004a; Rogers and Kaufman, 1996). Perturbations of *en* in *Drosophila* imaginal discs can cause mirror-image axis duplications and bifurcations (Tabata et al., 1995), similar to perturbations of Wg signaling (Jiang and Struhl, 1996; Johnston and Schubiger, 1996). Therefore, a hypothesis of functional conservation of both *wg* and *en* would predict that disruption of either gene should cause one or more of the following phenotypes: 1. Lack of *wg* activity should prevent the formation of appendage primordia, resulting in embryos lacking limbs. 2. *en*-depleted limbs may have AP axis defects because of a requirement for *en* in maintaining the posterior compartment. It is also possible that *en* activation of *wg* in *Oncopeltus* may persist in later stages; in which case, RNAi of either gene may also produce DV axis defects, such as paraxial outgrowth or mirror-image duplication. 3. *wg* RNAi should cause defects in differentiation along the PD limb axis. This could also be true of *en* RNAi, if the *en*–*wg* interaction were maintained at later stages.

RNA interference of *Oncopeltus en* caused defects in body segmentation and appendage development. Affected embryos were organized into three phenotypic classes, based on the degree of segmentation defects (Table 1). Mild class I individuals exhibited some poorly demarcated boundaries between abdominal tergites (Fig. 4F), which progressed into stronger class II defects in which thoracic and abdominal tergites were fused and poorly demarcated (Fig. 4G). In severe class III individuals, thoracic and abdominal body segments are not distinguishable (Fig. 4H). The abdomen is also reduced, suggesting that the development of germband segments from the growth zone may also be disrupted.

Interestingly, appendages in all *en*-depleted phenotypic classes bear similar defects. Antennae are severely deformed

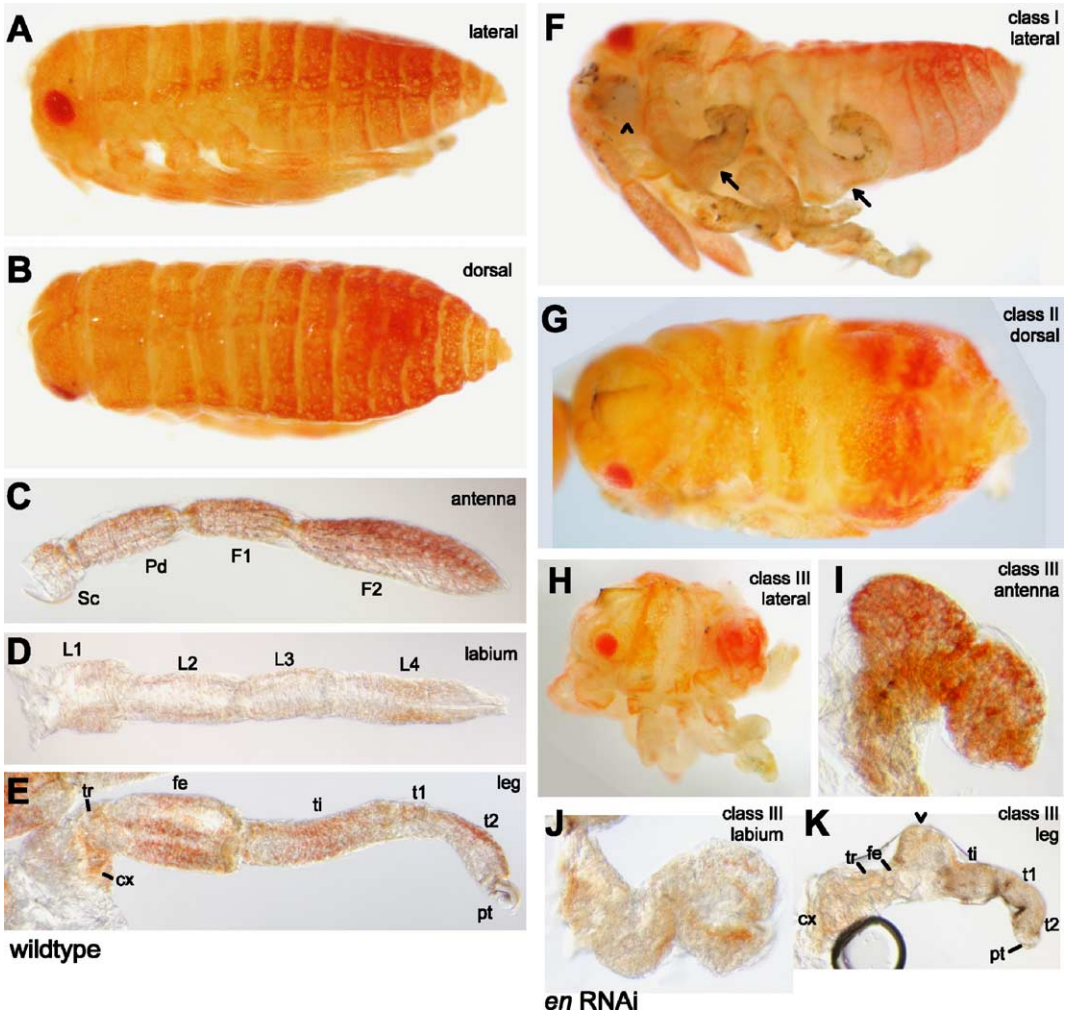

Fig. 4. Of'en RNAi causes defects in appendage development, segmentation, and dorsal closure. Wild type 8-day Oncopeltus embryos are shown just prior to hatching in (A) lateral and (B) dorsal aspects. (C) A wild type antenna from an embryo of this stage, which consists of four podomeres. (D) The labium is normally formed by the fusion of left and right embryonic appendages and becomes divided into four podomeres. (E) A wild type leg, distinct podomeres. (F) Lateral view of a mild class I *en*-depleted embryo. Note the curling of the legs (arrows) and the severely deformed labial appendage (arrowhead). (G) Dorsal view of a moderate class II embryo, showing a lack of distinguishable segment boundaries in the abdomen. (H) A severe class III *en*-depleted individual in lateral view. Notice that abdominal segments are reduced and extensively fused. All appendages are still present and bear similar defects in all classes. (I) The antenna of a class III *en*-depleted individual is severely deformed and missing two podomeres. (J) The labium from a similar embryo is severely deformed, such that individual podomeres cannot be identified. (K) Legs of *en*-depleted individuals are reduced, particularly in the tibia and more distal podomeres. The femur is partially bifurcated in the anterior direction (arrowhead), and the pretarsal claw is poorly formed. Abbreviations: cx, coxa; F1–F2, flagella I–II; fe, femur; L1–L4, labial podomeres 1–4 Pd, pedicel; pt, pretarsal claw; Sc, scape; t1–t2, tarsus 1–2; ti, tibia; tr, trochanter.

in some affected embryos, consisting of only two podomeres (Fig. 4I). These do not extend straight away from the head as do the normal antennae, and the second distal podomere joins the first close to its proximal joint with the head. This suggests defects in the PD axis and possibly also in the AP or DV axes. (It was not possible to determine the axes of orientation.) The feeding stylets, the appendicular derivatives of the mandibular and maxillary segments, could not be found in dissections of affected individuals (not shown). The labium appeared to be the most sensitive structure to *en* RNAi, showing distal defects in individuals without obvious germband defects (not shown). In most *en*-depleted embryos, the labium was reduced to a two-segmented structure (Fig. 4F, arrowhead; J). The mature *Oncopeltus* labium is formed by the mid-ventral fusion of separate left and right embryonic labial appendages. These appendages often failed to fuse in *en* RNAi. The legs of *en*-depleted embryos are deformed and swollen at the femur (Fig. 4F, arrows; K). This swelling is consistently found on the anterior side of the legs, and this may represent an incipient bifurcation of the limb axis (Fig. 4K, arrowhead). Legs are also reduced in size, particularly in the length of the tibia and more distal podomeres.

Expression of wingless

In *Oncopeltus*, we first examined *wg* expression in the blastoderm at 40 h. At this stage, *wg* is strongly expressed

in a crescent-shaped domain at the posterior of the egg (Figs. 5A–B). This is the presumptive site of germband invagination (Butt, 1949), and this expression persists later in the growth zone of the germband (Fig. 5D). Weak expression extends from the edges of this crescent domain laterally along the sides of the egg and ends at approximately 15% egg length (EL) in an area of slightly greater intensity (Fig. 5B). Two circumferential bands of weak expression can also be observed at approximately 30 and 55% EL (Figs. 5A–C). It is not clear what functional significance these domains may have nor whether they share homology to *wg* expression domains known from any other arthropods.

In the germband, *Oncopeltus wg* is expressed in segmentally iterated stripes. At 48 h, the germband has formed and consists of 6 segments. At this stage, *wg* expression can be seen in segmental stripes (Fig. 5D). This is similar to expression of *wg* in the embryo of *Drosophila* (Baker, 1988b). *Of'wg* expression is slightly anterior of cells known to express *engrailed* (Liu and Kaufman, 2004a; Rogers and Kaufman, 1997), although it is unclear whether expression of *wg* and *en* is mutually exclusive, as in the *Drosophila* germband (Ingham and Martinez-Arías, 1992). As noted, a separate domain of expression is seen in the growth zone of *Oncopeltus*, which persists throughout germband elongation.

After all body segments have been formed by 72 h, *wg* stripes fail to cross the ventral midline, except in the terminal segments: the ocular and A11 abdominal segment (Fig. 5E). Expression in appendage-bearing segments extends into the limbs (Fig. 5F). This pattern may be homologous to that seen for *wg* expression in *Drosophila* leg imaginal discs (Baker, 1988b; Campbell et al., 1993).

By 96 h of development, *wg* expression persists in the appendages and A11 but becomes less intense in other abdominal segments, where it is restricted to shortened stripes near the ventral midline, but interrupted at the midline itself (Fig. 5G). In the mandibular and maxillary appendages of *Oncopeltus*, *wg* expression is comparable to that in the thoracic and labial segments only at the distal tips, while proximal appendicular areas and the ventral body show comparatively lower levels of accumulation. This is most pronounced in the maxillary segment, where expression drops to undetectable levels in the proximal appendage buds and appears to be absent from the body in this segment. These unique details of *Of'wg* expression may be associated with the subtle differences in morphology between the mandibular and maxillary stylets. Interestingly,

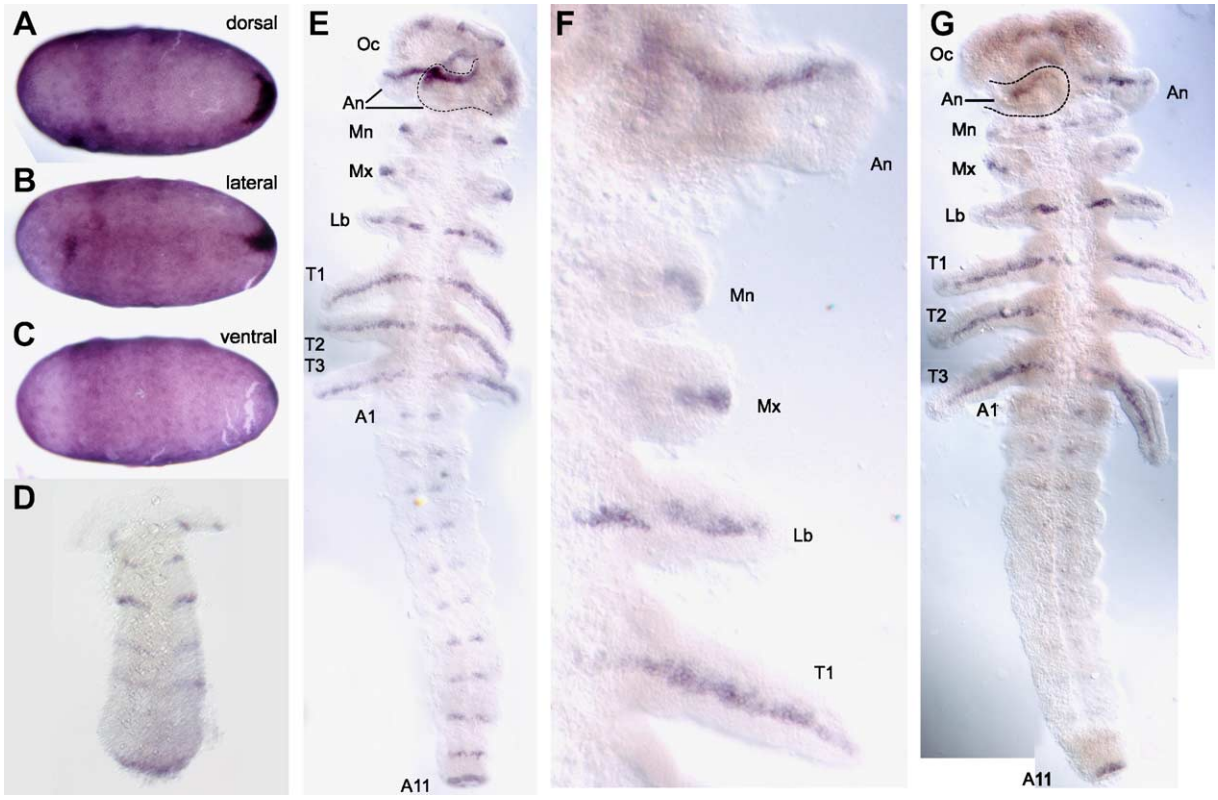

Fig. 5. Expression of Of'wg. (A–C) Of'wg expression in a 40 h blastoderm stage embryo appears throughout the embryo. It is most intense at the posterior site of germband invagination. (D) Expression in a 48 h germband embryo appears in segmental stripes. (E) Of'wg expression in a 72 h embryo extends into the appendages in a ventral stripe. At this stage, signal becomes weaker in the lateral regions of the abdominal segments. (F) Close-up of a 72 h embryo stained for Of'wg, showing antennal, mandibular, maxillary, labial, and first thoracic appendages. (G) Staining in an approximately 96 h embryo. Abbreviations: Oc, ocular segment; An, antennal segment; Mn, mandibular segment; Mx, maxillary segment; Lb, labial segment; T1–3, thoracic segments 1–3; A1–11, abdominal segments 1–11.

the labial *wg* stripe is interrupted near the base of the labial appendage bud, but the significance of this detail is unclear.

wg RNAi causes defects in body segmentation and eye development

Zygotic RNAi of *Oncopeltus wg* produced defects in dorsal segmentation and eye development, but unlike *en* RNAi, no discernible effect was seen in the appendages. Affected individuals failed to hatch and showed varying degrees of fusion in the abdominal tergites (Figs. 6A–C). Dorsal tissue was also striated in more mildly affected individuals (Fig. 6A), suggesting that dorsal closure also requires Wg activity. In severely affect individuals, abdominal tergites cannot be distinguished (Fig. 6C). However, the size of the abdomen is not reduced, in contrast to severe *en* phenotypic classes. The eyes of *wg*-depleted individuals are also much smaller than in the wild type. Despite these phenotypic defects, *wg* RNAi did not produce abnormalities in the appendages. Specific podomeres were clearly distinguishable along the PD axis, and no other defects could be found (Figs. 6D–E).

pan RNAi causes truncation of the germband

Because of the relatively mild phenotypes seen in *wg* RNAi, we also tested the role of Wnt signaling in *Oncopeltus* through analysis of the *pangolin* (*pan*) orthologue. *pan* and its orthologues in vertebrates encode a TCF family transcriptional activator (Brunner et al., 1997). To activate transcription, Pan must form a complex with the DNA-binding protein Armadillo (Arm), which accumulates in the nucleus as a result of Wg signal reception at the cell surface (reviewed by Bejsovec, 2005). Canonical Wg

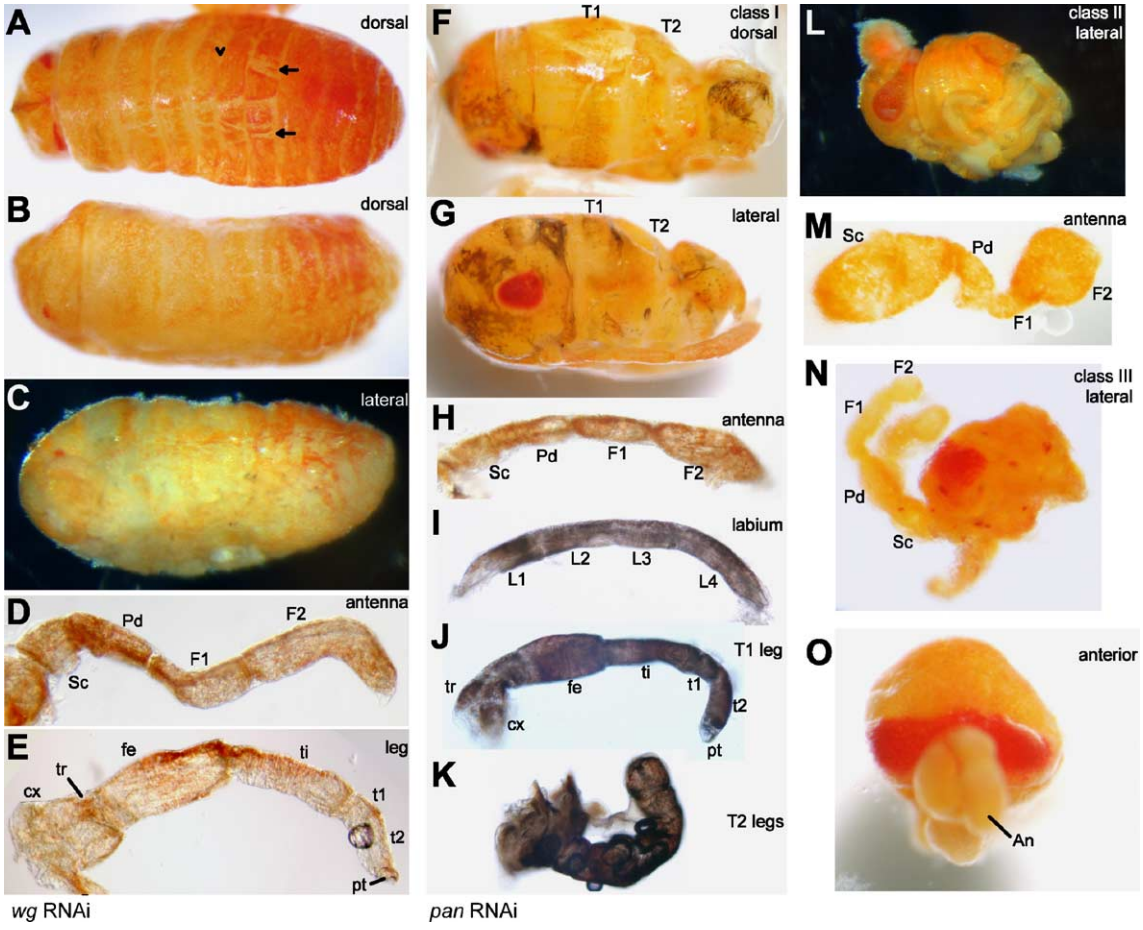

Fig. 6. wg and pan RNAi. (A) A dorsal view of a mildly affected Oncopeltus embryo depleted for wg. Abdominal tergites are poorly distinguished in places (arrowhead). Dorsal tissue is also striated, suggesting abnormalities in dorsal closure. (B) A dorsal view of a more strongly affected embryo. Notice that the size of the eyes is reduced. Segment boundaries in this individual are poorly delineated, and abdominal tergites appear to be fused. (C) Lateral view of a severely affected individual, in which the eyes are almost completely lost. Abdominal body segments also lack distinct boundaries and have begun to fuse. However, antennae (D) and legs (E) appear to be morphologically normal. (F) Dorsal view of a class I *pan*-depleted embryo. (G) Lateral view of the same embryo, showing that the body is truncated after the T2 segment. (H) Antenna, (I) labium, and (J) T1 leg of a class I *pan*-depleted embryo. These appendages are indistinguishable from those of wild type embryos just prior to hatching. (K) T2 legs of a class I *pan*-depleted embryo, which have fused along their posterior sides. (L) The body is reduced overall in a moderate class II *pan*-depleted embryo. (M) However, antennae remain properly patterned in this phenotypic class. (N) A severely affected class III embryo consists of only a head with identifiable eyes and properly patterned antennae. (O) A similar embryo viewed from the anterior shows that the eyes field extend dorsally and fuse in these embryos.

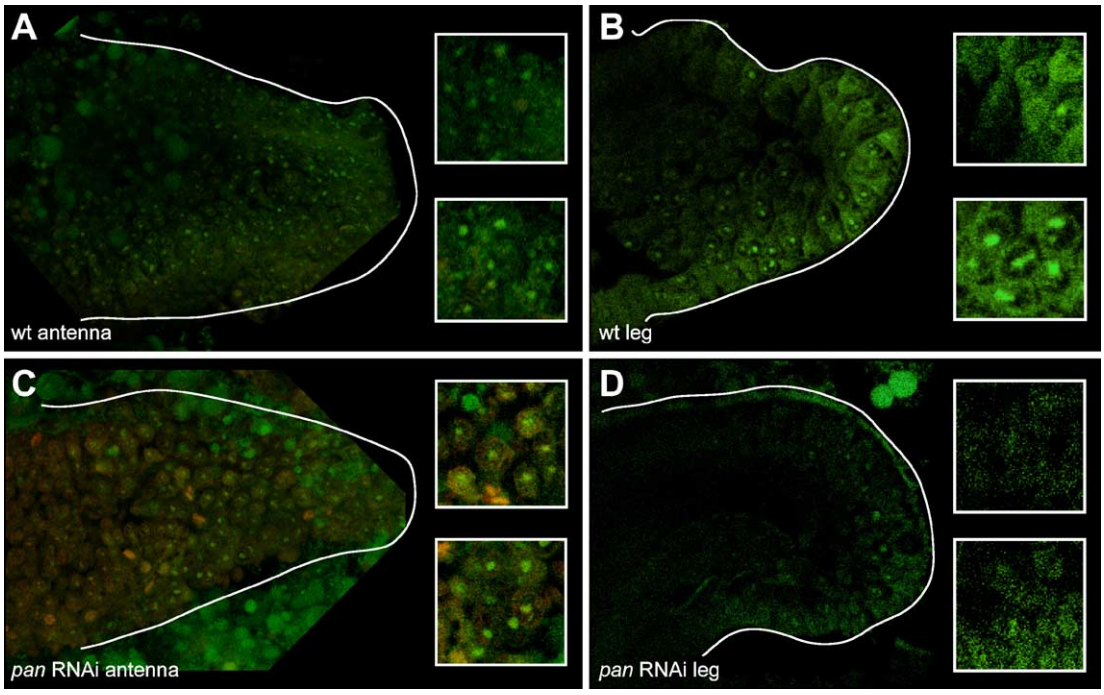

Fig. 7. pan RNAi disrupts nuclear localization of Arm protein in the posterior compartment of leg buds. All limbs are shown from a ventral aspect with distal to the right and anterior at the top. Arm antibodies are marked with FITC (green), and DNA is marked with TOTO-3 (red) as a counter-stain. Insets show a close-up of cells from the anterior (above) and posterior (below) sides of the limb. (A) Wild type (A) antennal and (B) leg buds at 62 h. (C) Antennal limb bud of a 120 h *pan*-depleted embryo in which nuclear localization of Arm appears throughout the appendage. (D) Leg bud of a similar pan-depleted embryo, showing that nuclear Arm localization is mostly absent from the posterior compartment.

signaling requires *pan* activity in a broadly conserved assemblage of organisms, and it is possible that other Wnt ligands may also require Pan activity.

In *Oncopeltus*, *pan* is expressed ubiquitously in the blastoderm and germband (not shown). Embryos produced through *pan* RNAi show a severe truncation of the germband. This phenotype is highly penetrant, with no wild type escapers obtained through maternal injections. We have grouped the range of phenotypic severity into three classes (Table 1). Class I contains the most mildly affected embryos. However, these are still characterized by the dramatic truncation of the embryo posterior of the second thoracic segment (Figs. 6F–G). The remaining body segments and structures appear fairly normal. Most interestingly, the appendages on these remaining segments are properly jointed and include distinct and appropriate podomeres. The antennae, mandibular and maxillary stylets, labium, and T1 legs appear normal (Figs. 6H–J). The T2 legs are fused medially at the posterior end of the embryo (Figs. 6F–G). These are the posterior-most structures of the embryo, and it appears that the legs are fused such that their posterior parasegmental compartments adjoin (Fig. 6K).

In more strongly affected class II embryos, the size of the body becomes reduced (Fig. 6L), and much of the egg yolk remains unincorporated by the embryo. However, the appendages remain properly patterned, although smaller, in proportion to the embryo (Fig. 6M). Class III embryos were the most severely affected by *pan* RNAi. They occupied a very small volume of the egg. In these individuals, segmentation of the body was not discernible, and embryos lacked obvious thoracic and abdominal structures (Fig. 6N). In these embryos, the eyes become fused medially across the dorsum of the head (Fig. 6O). In *Drosophila*, loss of the Wg signaling activity also produces ectopic omatidia in the dorsal head (Baonza and Freeman, 2002), and expression studies in *Schistocerca* have also suggested a conserved role for Wg signaling in the eyes of more basal insects (Dong and Friedrich, 2005). Significantly, even severe *pan*-depleted embryos bear antennae. In some individuals, they are fused medially at the anterior (Fig. 6O) but consist of four distinct podomeres (Fig. 6N).

Nuclear location of Arm protein is disrupted by pan RNAi

Because RNAi does not necessarily produce a null state, we wished to assess the degree to which Wnt signaling was disrupted. Wnt signaling leads to the nuclear accumulation of Armadillo (Arm) protein, which interacts with Pan to activate transcription of target genes, and this system is conserved in *Drosophila* as well as vertebrates (Bejsovec, 2005). Therefore, we made use of a broadly cross-reactive monoclonal Arm antibody (Riggleman et al., 1990) to compare the patterns of cells in which Wnt signaling was activated in the limb buds of *Oncopeltus* wild type and RNAi depletion embryos. This was done in a *pan*-depleted background since this yielded a more consistently strong phenotype, and depleted embryos could be obtained *en mass* from parental dsRNA injection.

Two outcomes could be expected in this experiment: First, based on the fact that Pan is known to act downstream of Arm, it might be predicted that no change in Arm localization would be caused by *pan* RNAi. However, maintenance of *wg* expression is dependent on autoregulation and feedback from signaling components in *Drosophila* (Hooper, 1994; Manoukian et al., 1995; Yoffe et al., 1995). Therefore, a second possibility is that *pan* RNAi would prevent the nuclear location of Arm as a result of the failure of *wg* autoregulatory maintenance.

In the leg buds of 62 h wild type embryos, Arm protein accumulates in the cytoplasm and nuclei of cells along the PD axis predominantly in the ventral posterior region (Fig. 7B). Nuclear localization was also seen in cells at the distal tip. This pattern of Arm nuclear localization is disrupted in embryos depleted for *pan*. Embryos used in this experiment fell into phenotypic class II, the group of moderately affected embryos in which the embryo was reduced but still produced thoracic body segments and legs. The leg buds of *pan*-depleted embryos did not show nuclear localization in the posterior compartment of the limb (Fig. 7D). Localization did persist somewhat at the distal tip of the legs.

Surprisingly, Arm is localized to nuclei of cells throughout the wild type antenna buds (Fig. 7A) in both compartments, although the intensity of nuclear staining in the anterior appears slightly weaker. This pattern remains unaffected by *pan* RNAi (Fig. 7C). This may suggest a fundamentally different function for Wnt signaling in the antennae as compared to the legs.

Expression of the appendage-patterning genes Distal-less and dachshund is not disrupted by Of pan RNAi

We have shown that in *Oncopeltus* Arm is not properly localized to nuclei in the limbs of *pan*-depleted embryos, indicating that Wnt signaling is being disrupted. However, appendage development is not affected by *pan* RNAi. Therefore, we also examined the expression of appendage-patterning genes, which are expressed at specific levels along the PD axis. In *Oncopeltus* and *Drosophila*, the expression of *Distal-less* (*Dll*) and *dachshund* (*dac*) appears in distal and medial limb podomeres, where they are required for growth and differentiation of those structures (Angelini and Kaufman, 2004). *Dll* and *dac* are positively regulated by Wg and Dpp signaling in the distal and medial regions, respectively, of the *Drosophila* imaginal leg discs (Abu-Shaar and Mann, 1998), and the topology model has predicted that this regulation would be conserved in other species.

Dll and *dac* expression was determined in a *pan* RNAi background through in situ hybridization. At early stages, *pan*-depleted embryos appear severely deformed, however appendages are readily identifiable. In embryos depleted for *pan* activity, *Dll* was expressed at the distal region of the antennae and in the telopodite of the legs (Fig. 8A). *dac* expression appeared in medial regions of appendages in *pan*-depleted embryos (Fig. 8B). These results suggest that normal levels of Wnt signaling are not required for activation of these genes along the PD axis of the appendages in *Oncopeltus*. These data are also consistent with phenotypic effects of *pan* and *wg* RNAi in *Oncopeltus*.

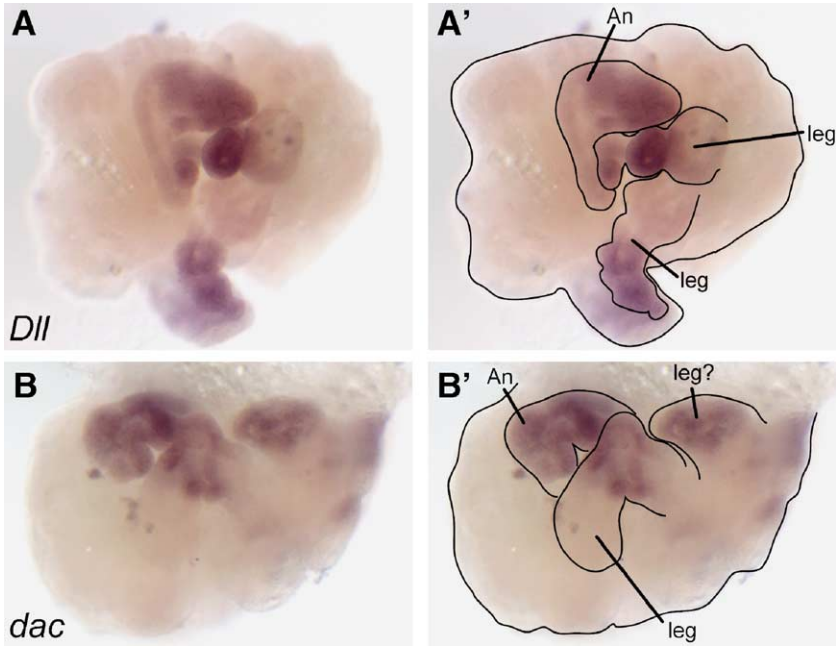

Fig. 8. Expression of appendage-patterning genes in *pan*-depleted embryos is not different from wild type. (A) Dll expression in a 120 h moderate class II *pan*-depleted embryo. Expression is seen in the distal regions of the antennae and legs. (B) dac expression in a similar embryo appears in the medial regions of the appendages. (A′, B′) Outlines of the embryos and appendages allowing easier visualization. These panels follow the usual convention: anterior is left, and dorsal is up. The mouthparts are obscured by the antennae and legs.

Discussion

Invagination and development of the germband

Oncopeltus is an intermediate-germband insect, in which three gnathal and three thoracic segments (mandibular through third thoracic) are patterned on the embryonic blastoderm, while the remaining body segments are added later anteriorly as well as posteriorly from the growth zone at the posterior of the germband (Butt, 1949; Liu and Kaufman, 2004a). The cells on the blastoderm at the site of germband invagination are similar to those of the growth zone, in that they continuously function in the production of new more posterior body segments until the proper number is reached and the growth zone ends its production of new segments. Both *dpp* and *wg* are strongly expressed on the *Oncopeltus* blastoderm at the site of germband invagination (Figs. 2A, 4B). In *dpp* RNAi, blastoderm cells condense at the posterior but are unable to form a germband through invagination of those cells (Figs. 3B–C).

In contrast, blastoderm cells invaginate and produce a germband in embryos for which Wnt signaling has been perturbed through *pan* RNAi. However, these embryos fail to properly add body segments from the growth zone. In particular, segments posterior of T2 seem to have an elevated requirement of normal levels of *pan* activity. (Presumably, this also indicates an elevated requirement for Wnt signaling function, although the Wnt ligand in question is not likely to be Wg since *wg*-depleted embryos develop with their posterior abdominal segments intact.) All segments posterior of T2 are deleted in even the mildest *pan*-depleted embryos scored (Fig. 6G). More anterior segments also have an apparent requirement for Wnt signaling, which can be seen in more strongly affected *pan* RNAi embryos. The most severe *pan* RNAi phenotypes retained the ocular, antennal, and at least one more posterior appendage-bearing segment (Fig. 6N). Therefore, these three anterior segments seem to have a lower requirement for Wnt signaling activity, if indeed any.

An intriguing possible explanation for these differences comes from a consideration of the origins of these segments. Segments derived from the growth zone, A1–A11, are among those with the highest requirement for Wnt signaling. Segments derived from the blastoderm fate map are generally more robust, despite Wnt signaling perturbation. The exception is the third thoracic segment, which is specified on the blastoderm, but also deleted in mild *pan* RNAi. However, cells that are part of this segment on the blastoderm will contribute to both T3 and the growth zone. Therefore, before germband invagination, the most posterior segment is not T3, but the precursor all segments posterior of T2. In this case, the elevated requirement for Wnt signaling activity may be common to all cells derived from this posterior region of the blastoderm. Interestingly, the truncation of the germband observed from *pan* RNAi in *Oncopeltus* is very similar to that described for *arm* RNAi in the cricket *G. bimaculatus* (Miyawaki et al., 2004). *Gryllus* and *Oncopeltus* share a similar blastoderm fate map, and *arm*-depleted *Gryllus* embryos are also truncated posterior of T2. Therefore, it seems likely that the role for Wnt signaling in the development of the germband is conserved among hemimetabolous insects.

Establishment of the limb PD axis in basal insects

In *Drosophila*, establishment of the appendage primordia and the limb PD axis requires Wg and Dpp pathway activity (Cohen et al., 1993; Gelbart, 1989). These ligands are transcribed in stripes along the anterior side of the disc AP compartment boundary, in ventral and dorsal territories, respectively. The ligands are thought to co-occur in the center of the disc, diminishing in a gradient more proximally. In this manner, cooperative activation and repression of target genes by Wg and Dpp signaling are responsible for the establishment and maintenance of the limb PD axis (Abu-Shaar and Mann, 1998; Theisen et al., 1996). This has been demonstrated by experiments showing that ectopic expression or loss of Wg or Dpp signaling components in the antennae or legs can produce mirror-image duplication of structures along the dorsal–ventral (DV) axis or bifurcation of the appendage in the DV plane (Jiang and Struhl, 1996; Johnston and Schubiger, 1996; Theisen et al., 1996).

However, studies of *wg* and *dpp* orthologues in more basal insect species have shown that, while *wg* expression is conserved, in a ventral stripe along the PD limb axis, *dpp* expression never appears in a PD stripe. Instead, as we have shown for *Oncopeltus dpp*, orthologues in basal insects are expressed broadly at early stages, narrow to a small distal region or ring near the distal tip and then elaborate into a more complex pattern of rings. These findings cast doubt on the universality of the mechanism of limb PD axis specification as known from *Drosophila* and suggest that the *Drosophila* mechanism is a derived state related to the development of the limbs from imaginal discs (Jockusch et al., 2000).

Alternatively, a model has recently been proposed which would explain the data from basal insects in the context of the *Drosophila* limb PD axis specification mechanism, using an argument of topology (Prpic et al., 2003). The topology model is based on several assumptions with testable hypotheses. First, its main assumption is that *wg* and *dpp* expression in basal insects is functionally homologous to that of *Drosophila*. This predicts that disruption of Wg or Dpp signaling in a primitive insect should produce appendage defects similar to defects found in *Drosophila*. Second, concurrent Wg and Dpp signaling activates and inhibits the same targets as in *Drosophila*. This predicts that reduction of Wg or Dpp signaling in a basal insect should also reduce the expression of distal domain genes, such as *Dll*. In this study, we have tested these hypotheses through RNA interference of Wg signaling

components in *Oncopeltus*, a hemimetabolous insect in which appendages develop from embryonic limb buds, and *wg* and *dpp* are expressed in the basal patterns.

Depletion of both *wg* and *pan* failed to produce defects in any of the appendages of *Oncopeltus* (Figs. 6A–O). In contrast, these embryos show severe defects in the eyes and dorsal ectoderm, tissues in which Wg signaling is also required in *Drosophila* (e.g., Baonza and Freeman, 2002; Ingham and Martinez-Arías, 1992). This combination of results was surprising. Therefore, we examined the orthologue of *engrailed*, another segment polarity gene with a well-conserved expression pattern. Depletion of *en* resulted in ectodermal defects similar to those seen in *wg* RNAi. However, *en* RNAi also produced defects in the PD and AP or DV axes of the appendages in *Oncopeltus*. These results support the idea that *en* is conserved in its segment polarity function between *Oncopeltus* and *Drosophila* and that establishment of the parasegment boundary is important to the proper development of the *Oncopeltus* appendages. It is interesting to consider then that our data suggest that specification of the parasegment boundary involves *wg* in the segmental ectoderm, but not in the appendages. Therefore, the first hypothesis of the topology model that perturbation of Wg signaling should produce appendage phenotypes similar to *Drosophila* is unsupported. Furthermore, in testing the second hypothesis of the topology model, we have shown that *Dll* and *dac* are expressed in wild type patterns in the appendage of *pan*-depleted embryos. Thus, that aspect of the model is also unsupported by the current results.

To confirm that Wnt signaling in the appendages is actually disrupted in *pan* RNAi, we examined Arm nuclear localization. In wild type embryos, cells in the posterior compartment of the legs have a greater frequency of high levels of nuclear Arm, while this pattern is disrupted in *pan* RNAi. Therefore, *pan* RNAi disrupts the AP pattern of Arm nuclear localization in the legs and presumably its ability to act as a transcriptional activator of Wnt signaling.

In summary, hypotheses arising from the topology model are not confirmed by tests in *Oncopeltus*. Therefore, the model cannot be accepted in its current form, and we must reconsider some of its assumptions. Our data have addressed the role of Wnt signaling in appendage development; however, we were not able to directly assess a role for Dpp in this process. Thus, it is possible that Dpp signaling does function in appendage development as predicted by the topology model. However, it must do so, either alone or in cooperation with a signaling pathway that does not include Pan and Arm. Unfortunately, the topology model does not explain how *dpp* expression becomes specified into the distal ring domain. It would seem such expression requires that PD information has already been established. Moreover, the bifurcation of the PD axis produced through *en* RNAi suggests that as in *Drosophila* the establishment of the AP axis must be a prerequisite to the proper regulation of genes specifying the PD axis.

The evolution of appendage patterning in insects

Our RNAi data for Wg signaling components in *Oncopeltus* are similar to phenotypes described for the germband of the cricket *Gryllus* (Miyawaki et al., 2004). *Oncopeltus* and *Gryllus* represent very distant hemimetabolous clades, therefore these results suggest that Wnt signaling functions described in *Oncopeltus* and *Gryllus* may represent the ancestral insect state. By extension, this implies that the role of *wg* in specification of the limb PD axis in *Drosophila* is a derived state.

Interestingly, a slightly different role for *wg* and *dpp* has been described in the appendages of *Tribolium* (Jockusch and Ober, 2004; Jockusch and Ober, in preparation). *Tribolium* is a holometabolous species in which larval antennae, legs, and mouthparts develop directly from embryonic limb buds, as in basal insects. RNA interference of *wg* in *Tribolium* causes a complete deletion of all appendages, except for the antennae, which are unaffected. Deletion of the appendages suggests a role for Wg signaling in specification of the appendage primordia, as in *Drosophila*, but unlike *Oncopeltus*. Additionally, *Tribolium dpp* is expressed in rings as in basal insects, but as in Oncopeltus *dpp* RNAi did not produce discernable appendage defects, although DV patterning of the germband was affected. Therefore, *Tribolium* appears to represent a third state, in which *wg* function is required in most but not all of the appendage types. This is intriguing since Arm localization in the antennae of *Oncopeltus* was unlike that in the legs, and it may be that patterning in the antennae of *Oncopeltus* and *Tribolium* (and perhaps basal insects in general) employs mechanisms distinct from other appendage types. This suggests that in the lineage leading to *Drosophila* the antennae were brought under the same regulatory mechanisms seen in other appendages (or vice versa).

It is noteworthy that, with the evolution of imaginal discs, the expression and developmental function of more downstream regulatory genes in the pathway have been well conserved. Regulatory genes such as *Dll*, *dac*, and *hth*, which specify the fates of specific PD domains, function similarly in the legs of all insects examined. The evolution of genes at this level seems to have been related more to specific morphologies, such as the extreme modification seen in mouthparts (Abzhanov et al., 2001; Angelini and Kaufman, 2004). The evolutionary transition from limb patterning in three-dimensional limb buds to two-dimensional imaginal discs can be considered as a topological issue. Therefore, it seems reasonable to assume that the underlying developmental genetic modification concurrent with this transition may have occurred in genes controlling specification of the limb axes.

If the PD axis is specified as a result of the AP and DV limb axes, as suggested by our *en* RNAi results, then PD domain genes are likely to be activated by a combination of genes expressed in separate AP or DV territories. Unfortunately, such genes remain to be identified and functionally

tested in basal insects. One possible route of investigation would be to identify activating transcription factors at conserved binding sites in the *cis*-regulatory regions of early PD domain genes, such as *Dll*. However, resolution of these issues must await future genomic and functional studies in basal insects.

Acknowledgments

The authors wish to thank Paul Z. Liu for cloning *Oncopeltus engrailed* and Jeana Stubbert for assistance in zygotic injections of *en* dsRNA. Thanks also to F. Rudolf Turner for his skill in electron microscopy. Equipment and facilities used in this work were partially supplied by the Indiana Genomics Initiative. We appreciate the comments of two anonymous reviewers, which helped improve the manuscript. DRA was supported by an NIH Genetics Training Grant (GM07757) and an NSF Integrative Graduate Education and Research Traineeship (DGE-9972830).

References

Abu-Shaar, M., Mann, R.S., 1998. Generation of multiple antagonistic domains along the proximodistal axis during *Drosophila* leg development. Development 125, 3821–3830.

Abzhanov, A., Kaufman, T.C., 2000. Homologs of *Drosophila* appendage genes in the patterning of arthropod limbs. Dev. Biol. 227, 673–689.

Abzhanov, A., Holtzman, S., Kaufman, T.C., 2001. The *Drosophila* proboscis is specified by two Hox genes, proboscipedia and Sex combs reduced, via repression of leg and antennal appendage genes. Development 128, 2803–2814.

Almirantis, Y., Papageorgiou, S., 1999. Modes of morphogen cooperation for limb formation in vertebrates and insects. J. Theor. Biol. 199, 235–242.

Angelini, D.R., Kaufman, T.C., 2004. Functional analyses in the hemipteran *Oncopeltus fasciatus* reveal conserved and derived aspects of appendage patterning in insects. Dev. Biol. 271, 306–321.

Angelini, D.R., Liu, P.Z., Hughes, C.L., Kaufman, T.C., submitted for publication. Hox gene functions and interactions in milkweed bug *Oncopeltus fasciatus* (Heteroptera). Dev. Biol.

Baker, N.E., 1988a. Transcription of the segment-polarity gene wingless in the imaginal discs of *Drosophila*, and the phenotype of a pupal–lethal wg mutation. Development 102, 489–497.

Baker, N.E., 1988b. Localization of transcripts from the wingless gene in whole *Drosophila* embryos. Development 103, 289–298.

Baonza, A., Freeman, M., 2002. Control of *Drosophila* eye specification by Wingless signalling. Development 129, 5313–5322.

Bejsovec, A., 2005. Wnt pathway activation: new relations and locations. Cell 120, 11–14.

Bejsovec, A., Martinez Arias, A., 1991. Roles of wingless in patterning the larval epidermis of *Drosophila*. Development 113, 471–485.

Brunner, E., Peter, O., Schweizer, L., Basler, K., 1997. pangolin encodes a Lef-1 homologue that acts downstream of Armadillo to transduce the Wingless signal in *Drosophila*. Nature 385, 829–833.

Butt, F.H., 1949. Embryology of the milkweed bug, *Oncopeltus fasciatus* (Hemiptera). Mem. -Cornell Univ. Agric. Exp. Stn. 283, 1–43.

Campbell, G.L., Caveney, S., 1989. engrailed gene expression in the abdominal segment of Oncopeltus: gradients and cell states in the insect segment. Development 106, 727–737.

Campbell, G., Weaver, T., Tomlinson, A., 1993. Axis specification in the developing *Drosophila* appendage: the role of wingless, decapentaplegic, and the homeobox gene aristaless. Cell 74, 1113–1123.

Cohen, B., Simcox, A.A., Cohen, S.M., 1993. Allocation of the thoracic imaginal primordia in the *Drosophila* embryo. Development 117, 597–608.

Diaz-Benjumea, F.J., Cohen, B., Cohen, S.M., 1994. Cell interaction between compartments establishes the proximal–distal axis of *Drosophila* legs. Nature 372, 175–179.

Dong, Y., Friedrich, M., 2005. Comparative analysis of Wingless patterning in the embryonic grasshopper eye. Dev. Genes Evol. 215, 177–197.

Gelbart, W.M., 1989. The decapentaplegic gene: a TGF-β homologue controlling pattern formation in *Drosophila*. Development 107, 65–74 (Suppl).

Hooper, J.E., 1994. Distinct pathways for autocrine and paracrine Wingless signalling in *Drosophila* embryos. Nature 372, 461–464.

Hughes, C.L., Kaufman, T.C., 2000. RNAi analysis of Deformed, proboscipedia and Sex combs reduced in the milkweed bug *Oncopeltus fasciatus*: novel roles for Hox genes in the Hemipteran head. Development 127, 3683–3694.

Ingham, P.W., Martinez-Arías, A., 1992. Boundaries and fields in early embryos. Cell 68, 221–235.

Irish, V.F., Gelbart, W.M., 1987. The decapentaplegic gene is required for dorsal–ventral patterning of the *Drosophila* embryo. Genes Dev. 1, 868–879.

Jiang, J., Struhl, G., 1996. Complementary and mutually exclusive activities of decapentaplegic and wingless organize axial patterning during *Drosophila* leg development. Cell 86, 401–409.

Jockusch, E.L., Ober, K.A., 2004. Hypothesis testing in evolutionary developmental biology: a case study from insect wings. J. Hered. 95, 382–396.

Jockusch, E.L., Nulsen, C., Newfeld, S.J., Nagy, L.M., 2000. Leg development in flies versus grasshoppers: differences in dpp expression do not lead to differences in the expression of downstream components of the leg patterning pathway. Development 127, 1617–1626.

Johnston, L.A., Schubiger, G., 1996. Ectopic expression of wingless in imaginal discs interferes with decapentaplegic expression and alters cell determination. Development 122, 3519–3529.

Kubota, K., Goto, S., Hayashi, S., 2003. The role of Wg signaling in the patterning of embryonic leg primordium in *Drosophila*. Dev. Biol. 257, 117–126.

Lawrence, P.A., Wright, D.A., 1981. The regeneration of segment boundaries. Philos. Trans. R. Soc. Lond., B Biol. Sci. 295, 595–599.

Lecuit, T., Cohen, S.M., 1997. Proximal–distal axis formation in the *Drosophila* leg. Nature 388, 139–145.

Liu, P.Z., Kaufman, T.C., 2004a. hunchback is required for suppression of abdominal identity, and for proper germband growth and segmentation in the intermediate germband insect *Oncopeltus fasciatus*. Development 131, 1515–1527.

Liu, P.Z., Kaufman, T.C., 2004b. Krüppel is a gap gene in the intermediate germband insect *Oncopeltus fasciatus* and is required for development of both blastoderm and germband-derived segments. Development 131, 4567–4579.

Manoukian, A.S., Yoffe, K.B., Wilder, E.L., Perrimon, N., 1995. The porcupine gene is required for wingless autoregulation in *Drosophila*. Development 121, 4037–4044.

Masucci, J.D., Miltenberger, R.J., Hoffmann, F.M., 1990. Pattern-specific expression of the *Drosophila* decapentaplegic gene in imaginal disks is regulated by 3' *cis*-regulatory elements. Genes Dev. 4, 2011–2023.

Miyawaki, K., Mito, T., Sarashina, I., Zhang, H., Shinmyo, Y., Ohuchi, H., Noji, S., 2004. Involvement of Wingless/Armadillo signaling in the posterior sequential segmentation in the cricket, *Gryllus bimaculatus* (Orthoptera), as revealed by RNAi analysis. Mech. Dev. 121, 119–130.

Nagy, L.M., Carroll, S., 1994. Conservation of wingless patterning functions in the short-germ embryos of *Tribolium castaneum*. Nature 367, 460–463.

Padgett, R.W., St. Johnston, R.D., Gelbart, W.M., 1987. A transcript from a

Drosophila pattern gene predicts a protein homologous to the transforming growth factor-β family. Nature 325, 81–84.

Prpic, N.M., Tautz, D., 2003. The expression of the proximodistal axis patterning genes Distal-less and dachshund in the appendages of *Glomeris marginata* (Myriapoda: Diplopoda) suggests a special role of these genes in patterning the head appendages. Developmental Biology 260, 97–112.

Prpic, N.-M., Janssen, R., Wigand, B., Klingler, M., Damen, W.G.M., 2003. Gene expression in spider appendages reveals reversal of exd/hth spatial specificity, altered leg gap gene dynamics, and suggests divergent distal morphogen signaling. Dev. Biol. 264, 119–140.

Riggleman, B., Schedl, P., Wieschaus, E., 1990. Spatial expression of the *Drosophila* segment polarity gene armadillo is posttranscriptionally regulated by wingless. Cell 63, 549–560.

Rijsewijk, F., Schuermann, M., Wagenaar, E., Parren, P., Weigel, D., Nusse, R., 1987. The *Drosophila* homolog of the mouse mammary oncogene int-1 is identical to the segment polarity gene wingless. Cell 50, 649–657.

Rogers, B.T., Kaufman, T.C., 1996. Structure of the insect head as revealed by the EN protein pattern in developing embryos. Development 122, 3419–3432.

Rogers, B.T., Kaufman, T.C., 1997. Structure of the insect head in ontogeny and phylogeny: a view from *Drosophila*. Int. Rev. Cytol. 174, 1–84.

Sanchez-Salazar, J., Pletcher, M.T., Bennett, R.L., Brown, S.J., Dandamudi, T.J., Denell, R.E., Doctor, J.S., 1996. The Tribolium decapentaplegic gene is similar in sequence, structure, and expression to the *Drosophila* dpp gene. Dev. Genes Evol. 206, 237–246.

Simcox, A.A., Roberts, I.J.H., Hersperger, E., Gribbin, M.C., Shearn, A., Whittle, J.R.S., 1989. Imaginal discs can be recovered from cultured embryos mutant for the segment-polarity genes engrailed, naked, and patched but not from wingless. Development 107, 715–722.

Svacha, P., 1992. What are and what are not imaginal discs: reevaluation of some basic concepts (Insecta Holometabola). Dev. Biol. 154, 101–117.

Tabata, T., Schwartz, C., Gustavson, E., Ali, Z., Kornberg, T.B., 1995. Creating a *Drosophila* wing de novo, the role of engrailed, and the compartment border hypothesis. Development 121, 3359–3369.

Theisen, H., Haerry, T.E., O'Connor, M.B., Marsh, J.L., 1996. Developmental territories created by mutual antagonism between Wingless and Decapentaplegic. Development 122, 3939–3948.

Yoffe, K.B., Manoukian, A.S., Wilder, E.L., Brand, A.H., Perrimon, N., 1995. Evidence for engrailed-independent wingless autoregulation in *Drosophila*. Dev. Biol. 170, 636–650.